Inorganic Chemistry

Article

pubs.acs.org/IC

Reactivity Studies of Oxo−Mo(IV) Complexes Containing Potential Hydrogen-Bond Acceptor/Donor Phenolate Ligands

Victor Wee Lin Ng, Michelle K. Taylor,† and Charles G. Young*

School of Chemistry, University of Melbourne, Victoria 3010, Australia

Supporting Information

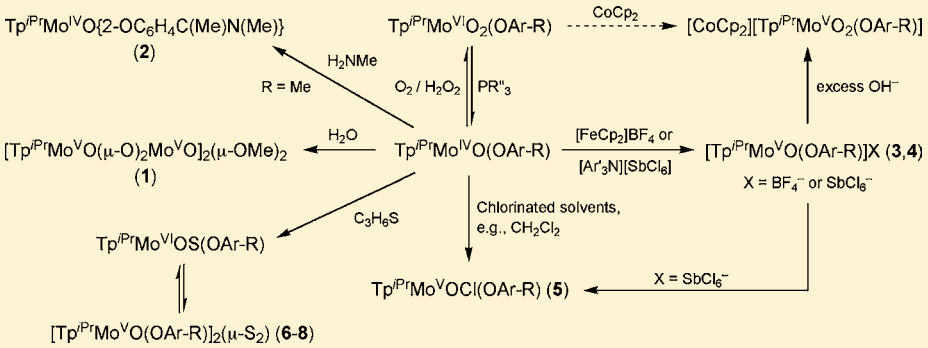

ABSTRACT: Reactivity studies of oxo−Mo(IV) complexes, $Tp^{iPr}MoO\{2\text{-}OC_6H_4C(O)R\text{-}\kappa^2O,O'\}$ (R = Me, Et, OMe, OEt, OPh, NHPh), containing chelated hydrogen-bond donor/acceptor phenolate ligands are reported. Hydrolysis/oxidation of $Tp^{iPr}MoO(2\text{-}OC_6H_4CO_2Ph\text{-}\kappa^2O,O')$ in the presence of methanol yields tetranuclear $[Tp^{iPr}MoO(\mu\text{-}O)_2MoO]_2(\mu\text{-}OMe)_2$ (**1**), while condensation of $Tp^{iPr}MoO\{2\text{-}OC_6H_4C(O)Me\text{-}\kappa^2O,O'\}$ and methylamine gives the chelated iminophenolate complex, $Tp^{iPr}MoO\{2\text{-}OC_6H_4C(Me)NMe\text{-}\kappa^2O,N\}$ (**2**), rather than the aqua complex, $Tp^{iPr}MoO\{2\text{-}OC_6H_4C(Me)NMe\text{-}\kappa O\}(OH_2)$. The oxo−Mo(IV) complexes are readily oxidized by dioxygen or hydrogen peroxide to the corresponding *cis*-dioxo−Mo(VI) complexes, $Tp^{iPr}MoO_2\{2\text{-}OC_6H_4C(O)R\}$; in addition, suitable one-electron oxidants, e.g., $[FeCp_2]BF_4$ and $[N(C_6H_4Br)_3][SbCl_6]$, oxidize the complexes to their EPR-active ($g_{iso} \approx 1.942$) molybdenyl counterparts (**3, 4**). Molybdenyl complexes such as $Tp^{iPr}MoOCl\{2\text{-}OC_6H_4C(O)R\}$ (**5**) and $Tp^{iPr}MoOCl_2$ also form when the complexes react with chlorinated solvents. The ester derivatives (R = OMe, OEt, OPh) react with propylene sulfide to form *cis*-oxosulfido−Mo(VI) complexes, $Tp^{iPr}MoOS\{2\text{-}OC_6H_4C(O)R\}$, that crystallize as dimeric μ-disulfido−Mo(V) species, $[Tp^{iPr}MoO\{2\text{-}OC_6H_4C(O)R\}]_2(\mu\text{-}S_2)$ (**6**−**8**). The crystal structures of $[Tp^{iPr}MoO(\mu\text{-}O)_2MoO]_2(\mu\text{-}OMe)_2$, $Tp^{iPr}MoO\{2\text{-}OC_6H_4C(Me)NMe\}$, $Tp^{iPr}MoOCl\{2\text{-}OC_6H_4C(O)NHPh\}\cdot\{2\text{-}HOC_6H_4C(O)NHPh\}$, and $[Tp^{iPr}MoO\{2\text{-}OC_6H_4C(O)R\}]_2(\mu\text{-}S_2)$ (R = OMe, OEt) are reported.

INTRODUCTION

The coordination chemistry of Mo(IV) is diverse and features a wide range of supporting ligands.[1−3] Complexes containing the $[Mo^{IV}O]^{2+}$ core are particularly interesting due to their involvement in stoichiometric and catalytic, 2-electron, atom transfer reactions. The bidirectional and catalytic oxygen atom transfer reactions of molybdenum typically interconvert dioxo−Mo(VI) and oxo−Mo(IV) centers, and many examples have been documented.[4−6] These reactions include the biologically important transformations performed by pterin-containing molybdenum enzymes, e.g., oxidation of sulfite to sulfate by sulfite oxidase and reduction of nitrate to nitrite by nitrate reductase.[7−9] The presence of *cis*-oxo(aqua)−Mo(IV) and *cis*-oxo(hydroxo)−Mo(V) centers in certain reduced molybdenum enzymes is supported by EXAFS studies[7−9] and the protein crystal structures of some enzymes, e.g., chicken liver sulfite oxidase[10] and *Pichia angusta* assimilatory nitrate reductase;[11] these centers are implicated in the regeneration of some Mo enzyme active sites,[7−9] and complexes of these types feature or are implicated in a number of model systems.[6,12−16] Many chemically important sulfur atom and nitrene group transfer reactions also involve oxo−Mo(IV) complexes.[17]

Recently, we reported mononuclear, oxo−Mo(IV) complexes of the type $Tp^{iPr}MoO\{2\text{-}OC_6H_4C(O)R\text{-}\kappa^2O,O'\}$ (**A**) containing a hydrotris(3-isopropylpyrazol-1-yl)borate ligand (Tp^{iPr}) and a phenolate ligand with the potential for hydrogen bonding (abbreviated as $^-OAr{-}R$ in Scheme 1 and the equations).[18] Incorporation of the phenolate ligands was aimed at stabilizing *cis*-oxo(aqua)−Mo(IV) complexes, $Tp^{iPr}MoO\{OC_6H_4C(O)R\text{-}\kappa O\}(OH_2)$, permitting their isolation and study as models for reduced molybdenum enzymes; chelation or κ^2O,O' coordination of the phenolate thwarted this aim. This paper describes the reactivity of the title complexes, explored with the aim of producing hitherto unreported *cis*-oxo(aqua)−Mo(IV) complexes and related Mo(V) species (Scheme 1). The reactions and products reported include reactions with water, oxygen, and methanol to give tetranuclear $[Tp^{iPr}MoO(\mu\text{-}O)_2MoO]_2(\mu\text{-}OMe)_2$ (**1**)

Received: December 11, 2011
Published: February 22, 2012

   dx.doi.org/10.1021/ic2026686 | *Inorg. Chem.* 2012, 51, 3202−3211

Scheme 1

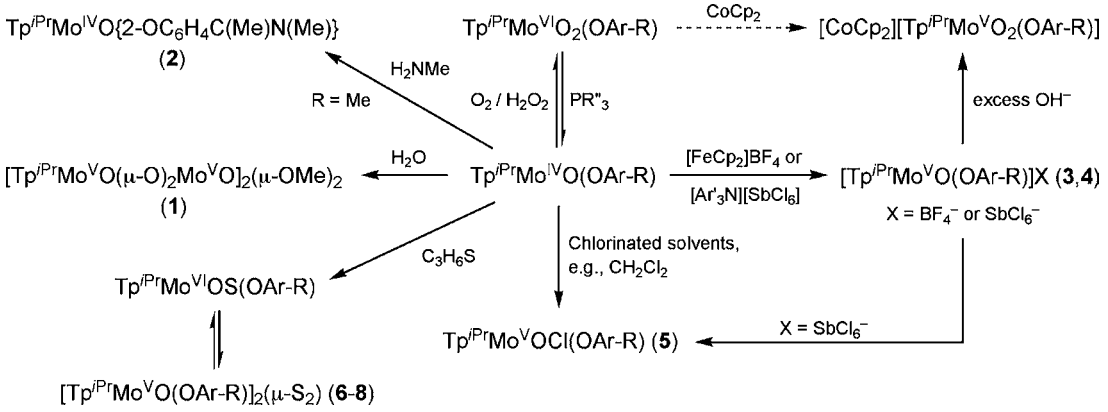

and related species; reaction of $Tp^{iPr}MoO\{2\text{-}OC_6H_4C(O)Me\}$ with methylamine to give the iminophenolate chelate complex, $Tp^{iPr}MoO\{2\text{-}OC_6H_4C(Me)NMe\text{-}\kappa^2O,N\}$ (**2**); reoxidation to the dioxo−Mo(VI) precursors; chlorine atom abstraction to form oxo−Mo(V) chloro species; oxidation by $[FeCp_2]BF_4$ (Cp = $\eta^5\text{-}C_5H_5^-$) or $[N(C_6H_4Br)_3][SbCl_6]$ to give, inter alia, $[Tp^{iPr}MoO\{2\text{-}OC_6H_4C(O)R\}][SbCl_6]$ (R = OMe (**3**), Me (**4**)) and $Tp^{iPr}MoOCl\{2\text{-}OC_6H_4C(O)NHPh\}.\{2\text{-}HOC_6H_4C\text{-}(O)NHPh\}$ (**5**); and sulfur atom abstraction from propylene sulfide to give $Tp^{iPr}MoOS\{2\text{-}OC_6H_4C(O)R\}$, isolated as dimeric $[Tp^{iPr}MoO\{2\text{-}OC_6H_4C(O)R\}]_2(\mu\text{-}S_2)$ (R = OMe (**6**), OEt (**7**), OPh (**8**), hereafter the 2-substituent designator will be excluded).

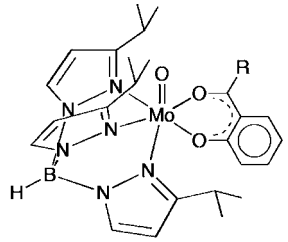

(**A**): R = Me, Et, OMe, OEt, OPh, NHPh

EXPERIMENTAL SECTION

Materials and Methods. All reactions were performed under an atmosphere of dinitrogen using dried, deoxygenated solvents, but work-ups were performed in air. The complexes, $Tp^{iPr}MoO\{2\text{-}OC_6H_4C(O)R\}$, were prepared as previously described.[18] Other chemicals were obtained from Aldrich Chemical Co. and used without purification.

Infrared spectra were recorded on a Bio-Rad FTS 165 FTIR spectrophotometer as pressed KBr disks. Electrospray ionization mass spectrometric (ESI-MS) experiments were carried out using a Micromass Quattro II mass spectrometer using samples dissolved in MeCN. NMR spectra were recorded at room temperature on Varian Unity-Plus 400 MHz or Inova 500 MHz spectrometers. Spectra were referenced to residual solvent peaks (for C_6D_6, δ_H 7.16, δ_C 128.0; for $CDCl_3$, δ_H 7.27). EPR spectra were recorded on a Bruker ECS 106 EPR spectrometer using 1,2-diphenyl-2-picrylhydrazyl as reference. Cyclic voltammograms were recorded using a 2 mm glassy carbon working electrode, platinum counter electrode, and a freshly prepared double-jacketed $Ag/AgNO_3$ reference electrode (10 mM $AgNO_3$ in MeCN with 0.1 M $NBu^n_4PF_6$ and clean silver wire) connected to an Autolab Potentiostat operated by the General Purpose Electrochemical System software (version 4.9). Samples were prepared as 1−2 mM solutions in MeCN with 0.1 M $NBu^n_4PF_6$ as supporting electrolyte. Scan rates were varied over the range 10−500 mV s^{-1}. Potentials were referenced against the ferrocene (Fc) couple, Fc^+/Fc, and are reported relative to the saturated calomel electrode (SCE). The Fc^+/Fc couple was set to the reported value of +0.400 V vs SCE for acetonitrile/0.1 M $NBu^n_4PF_6$ solutions.[19] Microanalyses were performed by Atlantic Microlab Inc., Norcross, GA.

Syntheses and Characterization Data. *Reactions with Water: Synthesis of 1.* The procedure below was adopted for all complexes: Green/purple $Tp^{iPr}MoO\{OC_6H_4C(O)R\}$ (ca. 60−70 mg, ∼0.1 mmol) was dissolved in THF (10 mL), and water (100 μL, ∼5.6 mmol) was added via an airtight syringe. The reaction mixture was stirred for 7 days and monitored by ^1H NMR. The color of the reaction mixtures remained unchanged, except for the reaction involving $Tp^{iPr}MoO(OC_6H_4CO_2Ph)$, which assumed a yellow-brown coloration. ^1H NMR monitoring indicated that all complexes except $Tp^{iPr}MoO(OC_6H_4CO_2Ph)$ were stable toward water. In the case of the reaction involving the phenyl ester, the residue obtained upon evaporation was redissolved in dichloromethane, layered with methanol, and stored at 4 °C. After several days, red crystals of **1** were obtained. Some colorless crystals of phenyl salicylate were also obtained (characterized by IR/NMR). Anal. Calcd for $C_{38}H_{62}B_2Mo_4N_{12}O_{10}$: C, 36.44; H, 4.99; N, 13.42. Found: C, 36.75; H, 5.03; N, 13.50. IR (KBr, cm^{-1}): 2968 m, 2929 w, 2870 w, ν(BH) 2488 w and 2454 w, 1632 br, ν(CN) 1510 s, 1402 m, 1387 m, 1362 m, 1195 vs, 1054 vs, ν(Mo═O) 983 vs and 950 s, ν(Mo−O−Mo) 767 and 736 s, 565 m, ν(Mo−O−Mo) 467 s. ^1H NMR ($CDCl_3$): δ_H 7.79 (4H, d, J = 2.0 Hz), 7.42 (2H, d, J = 2.0 Hz), 6.31(4H, d, J = 2.0 Hz), 5.84 (2H, d, J = 2.0 Hz), 3.82−3.86 (8H, overlapping peaks), 3.66 (4H, sept, J = 7.2 Hz), 1.88 (12H, m, overlapping peaks), 1.38 (12H, m, overlapping peaks), 1.22 (12H, m, overlapping peaks). ESI-MS: 1224.6 $[M - 2CH_3 + H]^+$ (1224.8), 612.2 $[M - 2CH_3 + 2H]^{2+}$ (612.04).

Reaction with Methylamine: Synthesis of 2. A green solution of $Tp^{iPr}MoO\{OC_6H_4C(O)Me\}$ (0.5 g, 0.85 mmol) in acetonitrile (50 mL) was treated with a solution of methylamine (33% in ethanol, 0.16 mL, 0.13 mmol) and stirred for 1 h. The resultant purple solution was reduced to dryness, and the residue was triturated with hexane to yield purple **2**, which was collected by filtration and recrystallized by slow cooling of a hot acetonitrile solution. The sample for microanalysis was dried under vacuum for 24 h. Yield 0.43 g (84%). Anal. Calcd for $C_{27}H_{38}BMoN_7O_2$: C, 54.10; H, 6.39; N, 16.36. Found: C, 53.87; H, 6.40; N, 16.39. IR (KBr, cm^{-1}): ν(BH) 2477 and 2447 m; ν(C═N) 1599 s; ν(CN) 1508 s; ν(Mo═O) 953 s. ^1H NMR (C_6D_6): δ_H 7.62 (1H, d, J = 2.4 Hz), 7.46 (1H, d, J = 2.4 Hz), 7.26 (1H, d, J = 2.4 Hz), 7.22 (1H, m, Ar), 7.0−7.2 (2H, m, Ar), 6.43 (1H, m, Ar), 6.16 (1H, d, J = 2.4 Hz), 5.92 (1H, d, J = 2.4 Hz), 5.80 (1H, d, J = 2.4 Hz), 3.81 (1H, sept, J = 6.8 Hz), 3.79 (1H, sept, J = 6.8 Hz), 3.38 (1H, sept, J = 6.8 Hz), 2.98 (3H, s, NCH_3), 1.75 (3H, s, $C(=N)CH_3$), 1.48 (3H, d, J = 6.8 Hz), 1.40 (3H, d, J = 6.8 Hz), 1.25 (6H, d, J = 6.8 Hz), 1.22 (3H, d, J = 6.8 Hz), 1.11 (3H, d, J = 6.8 Hz). $^{13}C\{^1H\}$ NMR (C_6D_6): δ_C 170.3, 170.0, 164.9, 163.8, 162.5, 138.0, 137.7, 134.3,

dx.doi.org/10.1021/ic2026686 | Inorg. Chem. 2012, 51, 3202−3211

134.0, 131.5, 127.5, 121.8, 116.1, 102.7, 102.5, 101.2, 48.5 (NCH_3), 29.5, 27.6, 27.2, 25.1, 25.0, 24.7, 24.0, 23.1, 22.6, 18.4 ($C(=N)CH_3$). ESI-MS: 599.4 $[M - 2H]^+$ (599.21). Cyclic voltammetry: $E_{1/2} = -0.078$ V (reversible, Mo^V/Mo^{IV}).

Reactions with Hydrogen Peroxide. The following procedure was adopted for all derivatives. A sample of $Tp^{iPr}MoO\{OC_6H_4C(O)R\}$ (ca. 30−35 mg, ∼0.05 mmol) was dissolved in 5 mL of dry deoxygenated THF, and hydrogen peroxide (30%, 5 drops) was added by syringe. The color of the reaction mixture turned from green/purple to orange/yellow immediately. A sample of the reaction mixture was compared to the corresponding *cis*-dioxo−Mo(VI) counterpart[20] using thin layer chromatography (in 1:2 THF/hexane). All TLC experiments indicated the presence of the oxidized product as the major (or sole) product.

Reactions with Dichloromethane. The following procedure was adopted for all derivatives. A sample of $Tp^{iPr}MoO\{OC_6H_4C(O)R\}$ (ca. 6−7 mg, ∼0.01 mmol) was dissolved in dichloromethane (1 mL) and filtered into an anaerobic EPR tube for analysis. The progress of the reaction was monitored by EPR spectroscopy. Initial EPR spectra were devoid of signals, but a signal at ca. $g_{iso} \approx 1.939$ slowly appeared. Over time, a second signal, ascribed to $Tp^{iPr}MoOCl_2$[21] ($g_{iso} = 1.949$), grew in intensity at the expense of the initial signal.

Reactions with Ferrocenium Tetrafluoroborate. The following procedure was adopted for all derivatives: A sample of $Tp^{iPr}MoO\{OC_6H_4C(O)R\}$ (ca. 6−7 mg, ∼0.01 mmol) and $[FeCp_2]BF_4$ (ca. 14 mg, ∼0.05 mmol) was dissolved THF/acetonitrile (10:1, 1 mL) and quickly filtered into an anaerobic EPR tube for analysis. Initial EPR measurements revealed a single peak at $g_{iso} \approx 1.942$, which was ascribed to the presence of $[Tp^{iPr}MoO\{OC_6H_4C(O)R\}]BF_4$. Subsequent reaction with deoxygenated water resulted in no change to the initial signal. However, when excess NBu^n_4OH (in methanol) was introduced, the peak at $g_{iso} \approx 1.942$ collapsed, giving rise to a broad signal at $g_{iso} \approx 1.907$, assigned to the corresponding *cis*-dioxo−Mo(V) radical anion.[14] A stoichiometric equivalent of the base failed to elicit an observable reaction.

Reactions with Ammoniumyl Hexachloroantimonate. The procedure below was adopted for the synthesis of **3**, **4**, and **5**; specific conditions or variations are indicated prior to each set of characterization data. To a mixture of $Tp^{iPr}MoO\{OC_6H_4C(O)R\}$ (0.50 g, ∼0.8 mmol) and $[N(4\text{-}C_6H_4Br)_3][SbCl_6]$ (0.60 g, 0.74 mmol) was added dichloromethane (5 mL) and toluene (10 mL). The reaction mixture immediately turned bluish-brown. After ca. 2 h, the brown solution was evaporated to dryness and the residue was extracted with toluene to remove excess starting material. The brown residue was then filtered, washed with toluene (2 × 5 mL), and dried under vacuum. Golden-brown, air-sensitive microcrystalline solids were obtained for **3** and **4**.

Complex ***3***. Reaction time 2 h, yield 0.43 g (63%). EPR (THF/MeCN): 298 K $\langle g_{iso} \rangle$ 1.942. IR (KBr, cm^{-1}): 3140 w, 2972 m, 2930 w, 2873 w, ν(BH) 2516 w and 2465 w-sh, ν(C=O) 1603 s, 1574 vs, 1536 vs, ν(CN) 1506 s, 1498 s, 1470 s, 1458 s, 1427 w, 1400 m, 1386 m, 1367 vs, 1327 w, 1288 w, 1229 s, 1192 s, 1162 w, 1147 w, 1105 w, 1087 w, 1065 m, 1049 m, 1031 w, ν(Mo=O) 960 s, 877 w, 846 m, 804 m, 793 s, 759 s, 731 s, 704 w, 670 w, 645 m, 464 w, 412 w. ESI-MS: 604.3 $[M]^+$ (604.20); 334.8 $[A]^-$ (334.71).

Complex ***4***. Reaction time 2 h, yield 0.58 g (74%). EPR (THF/MeCN): 298 K $\langle g_{iso} \rangle$ 1.941. IR (KBr, cm^{-1}): 3139 w, 2971 m, 2928 w, 2872 w, ν(BH) 2519 w; ν(C=O) 1603 s; 1562 vs, 1519 vs, ν(CN) 1505 vs; 1463 m, 1396 s, 1387 s, 1365 s, 1319 w, 1290w, 1278 w, 1224 s, 1192 vs, 1161 m, 1139 m, 1086 m, 1070 s, 1062 s, 1046 m, 1030 w, 981 w, ν(Mo=O) 963 s, 867 m, 804 m, 793 m, 750 s, 732 s, 713 w, 648 m, 620 m, 561 w, 450 w. ESI-MS: 588.3 $[M]^+$ (588.19); 334.7 $[A]^-$ (334.71).

Complex ***5***. Yield 0.33 g (48%). Anal. Calcd for $C_{44}H_{49}BMoN_8O_5Cl$: C, 57.94; H, 5.42; N, 12.29. Found: C, 57.55; H, 5.40; N, 12.40. EPR (THF/MeCN): 298 K $\langle g_{iso} \rangle$ 1.939. IR (KBr, cm^{-1}): ν(NH) 3296 s, 3139 w, 3113 w, 3067 w, 2974 m, 2929 w, 2871 w, ν(BH) 2510 w, ν(C=O) 1668 and 1651 s, 1600 s, 1592 s, 1542 s, ν(CN) 1502 vs, 1470 s, 1450 s, 1339 m, 1385 s, 1365 m, 1323 s, 1285 m, 1282 m, 1255 w, 1219 s, 1191 vs, 1159 m, 1083 m, 1072 s, 1048 s, ν(Mo=O) 967 s, 904 m, 857 m, 828 w, 793 m, 783 s, 759 s, 748 m, 730 s, 714 w, 688 m, 670 w, 620 m, 580 w, 506 w, 460 w. ESI-MS: 700.4 $[M - L]^+$ (700.19), 665.4 $[M - L - Cl]^+$ (665.22), 591.2 $[M - L - C_6H_9N_2]^+$ (591.11) (L = $HOC_6H_4C(O)NHPh$).

Reactions with Propylene Sulfide: Synthesis of ***6***−***8***. The following procedure was adopted for all three derivatives. A purple suspension of $Tp^{iPr}MoO\{OC_6H_4C(O)R\}$ (R = OMe, OEt, OPh) (1.0 g, ca. 1.5 mmol) in acetonitrile (10 mL) was treated with excess propylene sulfide (400 μL, 5.10 mmol) and stirred for 14 h. The reaction mixture was briefly cooled to −30 °C and then filtered to yield a red-brown microcrystalline solid that was washed with cold, dry hexane and dried in vacuo. The complexes were purified by recrystallization from a mixture of THF/*n*-hexane or toluene/*n*-hexane.

Complex ***6***. Yield: 0.76 g (72%). Anal. Calcd for $C_{26}H_{35}BMoN_6O_3S$: C, 49.22; H, 5.56; N, 13.25; S, 5.05. Found: C, 49.36; H, 5.78; N, 13.20; S, 5.00. IR (KBr, cm^{-1}) (values in parentheses for monomer): 2970 s, 2928 m, 2869 m, ν(BH) 2486 and 2459 m, ν(C=O) 1706 vs (1733 s), 1594 m, 1564 w, ν(CN) 1508 vs, 1474 s, 1450 vs, 1431 w, 1398 m, 1385 s, 1364 m, 1305 vs, 1254 s, 1238 s, 1195 vs, 1157 w, 1127 m, 1104 w, 1092 w, 1080 m, 1070 s, 1048 vs, 1025 w, ν(Mo=O) 936 s (917 s), 890 s, 815 m, 796 m, 779 s, 757 s, 732 vs, 701 w, 674 m, 623 m, (ν(Mo=S) 485 m), 423 w. ^{1}H NMR ($CDCl_3$): δ_H 7.86 (1H, d, J = 7.2 Hz, Ar), 7.67 (1H, d, J = 2.4 Hz), 7.66 (1H, d, J = 2.4 Hz), 7.52 (1H, d, J = 2.4 Hz), 7.00 (2H, apparent br s, Ar), 6.15 (2H, apparent t, overlapping peaks), 5.93 (1H, d, J = 2.4 Hz), 4.59 (1H, sept, $J \approx 6.4$ Hz), 3.64 (1H, sept, $J \approx 6.9$ Hz), 3.55 (1H, br s), 2.55−3.20 (4H, overlapping peaks), 1.26 (6H, apparent t, overlapping peaks), 1.20 (3H, d, J = 6.8 Hz), 0.94 (3H, d, J = 6.8 Hz), 0.89 (3H, br s), 0.76 (3H, br s). Several peaks were missing due to fluxional behavior. ESI-MS: 636.4 $[M]^+$ (636.16) (dimer not observed in solution). Cyclic voltammetry: $E_{1/2} = -0.461$ V (reversible, Mo^{VI}/Mo^V).

Complex ***7***. Yield: 0.72 g (68%). Anal. Calcd for $C_{27}H_{37}BMoN_6O_4S$: C, 50.01; H, 5.75; N, 12.96; S, 4.94. Found: C, 49.61; H, 5.64; N, 12.91; S, 4.80. IR (KBr, cm^{-1}) (values in parentheses for monomer): 2972 m, 2928 m, 2870 w, ν(BH) 2490 w and 2459 w, ν(C=O) 1702 s (1691 s), 1592 m, 1562 w, ν(CN) 1509 s, 1494 m, 1473 m, 1446 s, 1396 s, 1385 s, 1365 m, 1301 vs, 1250 s, 1237 s, 1195 s, 1155 m, 1125 m, 1092 m, 1080 m, 1070 s, 1048 s, 1025 w, ν(Mo=O) 935 s (917 s), 892 m, 840 w, 819 w, 796 m, 779 m, 756 m, 733 s, 704 w, 669 w, 618 m, 558 w, 531 w, 515 w, 495 w, (ν(Mo=S) 484 m), 422 w. ^{1}H NMR ($CDCl_3$): δ_H 7.93 (1H, br d, Ar), 7.66 (2H, br d, overlapping peaks), 7.51 (1H, d, J = 2.4 Hz), 7.37 (1H, br m, Ar), 7.04 (1H, br m, Ar), 6.15 (2H, apparent t, overlapping peaks), 5.94 (1H, br s), 4.58 (1H, br m), 3.30−4.00 (3H, m, overlapping peaks), 2.98 (1H, br m), 1.10−1.40 (∼10H, m, overlapping peaks), 0.70−1.00 (∼10H, m, overlapping peaks). Several peaks were missing due to fluxional behavior. ESI-MS: 650.2 $[M]^+$ (650.18) (dimer not observed in solution). Cyclic voltammetry: $E_{1/2} = -0.475$ V (reversible, Mo^{VI}/Mo^V).

Complex ***8***. Yield: 0.61 g (60%). Anal. Calcd for $C_{31}H_{37}BMoN_6O_4S$: C, 53.46; H, 5.35; N, 12.07; S, 4.60. Found: C, 53.13; H, 5.65; N, 11.81; S, 4.81. IR (KBr, cm^{-1}) (values in parentheses for monomer): 2968 m, 2928 m, 2871 w, ν(BH) 2494 w and 2459 w, ν(C=O) 1720 s (1745 s), 1592 m, 1562 w, ν(CN) 1506 m, 1492 m, 1469 s, 1446 s, 1396 m, 1385 s, 1364 m, 1298 vs, 1251 s, 1191 vs, 1155 m, 1114 m, 1080 m, 1069 m, 1049 s, 1037 m, ν(Mo=O) 943 s (917 s), 880 m, 841 w, 816 w, 793 w, 782 w, 753 m, 735 m, 730 m, 702 w, 688 m, 670 w, 612 m, 495 w, (ν(Mo=S) 484 m). ^{1}H NMR ($CDCl_3$): δ_H 7.96 (1H, d, J = 7.2 Hz, Ar), 7.65 (2H, apparent d, overlapping peaks), 7.33 (2H, overlapping peaks), 6.90−7.20 (3H, br m, overlapping peaks, Ar), 6.12 (3H, apparent d, overlapping peaks), 5.70 (1H, br s), 4.56 (1H, br m), 4.35 (br m, possibly second isomer), 3.56 (1H, br m), 3.05 (1H, br m), 2.90 (br m, possibly second isomer), 2.62 (br m, possibly second isomer), 1.20−1.40 (8H, overlapping peaks), 0.80−1.00 (8H, overlapping peaks). Several peaks were missing, while extra sets of methine C*H* peaks (of Tp^{iPr}) were observed due to fluxional behavior. ESI-MS: 699.3 $[M + H]^+$ (699.18) (dimer not observed in solution). Cyclic voltammetry: $E_{1/2} = -0.450$ V (reversible, Mo^{VI}/Mo^V).

dx.doi.org/10.1021/ic2026686 | *Inorg. Chem.* 2012, 51, 3202−3211

X-ray Crystallography. Crystallographic data are summarized in Table 1. Crystals of **2**·2CH_2Cl_2 were obtained by allowing methanol to diffuse into a dichloromethane solution of the reaction residue; the unit cell of this compound contains two (independent) molecules of complex and four molecules of dichloromethane. Crystals of **2**·3MeCN and **5** were obtained from slow evaporation of acetonitrile and hexane solutions of the complexes, respectively. Crystals of **6** and **7**·C_7H_8 were obtained from slow diffusion of hexane into toluene solutions of the complexes. Crystals were coated in mineral oil and mounted on glass fibers. X-ray diffraction data to $2\theta = 55°$ were collected on a Bruker CCD area detector at 130 K using Mo Kα radiation (0.71073 Å). Cell parameters were acquired by the SMART software package, and data reduction was performed using SAINT. Structures were solved by direct methods (SHELXS-97[22]) and refined using full-matrix least-squares on F^2 (SHELXL-97).[23] Structural drawings were generated using ORTEP-3.[24] All non-hydrogen atoms were included in difference maps, and anisotropic parameters were employed. Hydrogen atoms were included in calculated positions.

RESULTS AND DISCUSSION

Reactions with Water. Conversion of the title complexes to oxo(aqua)−Mo(IV) complexes via reaction with water was investigated. However, most were found to be stable in the presence of deoxygenated water over several days. The ester derivatives underwent hydrolysis and adventitious oxidation, resulting in formation of polynuclear molybdenum complexes, over extended reaction periods. The tetranuclear oxo−Mo(V) complex, $[Tp^{iPr}MoO(\mu\text{-}O)_2MoO]_2(\mu\text{-}OMe)_2$ (**1**), was isolated following hydrolysis/oxidation of $Tp^{iPr}MoO(OC_6H_4CO_2Ph)$ in the presence of methanol.

The crystal structure of the bis(dichloromethane) solvate of **1** was determined by X-ray diffraction. Tetranuclear **1** (Figure 1) has a centrosymmetric structure comprised of two identical dinuclear Mo(V) moieties connected by two bridging methoxide ligands.

Table 1. Crystallographic Data

parameter	**1**·2CH_2Cl_2	**2**·3MeCN	**5**	**6**	**7**·C_7H_8
formula	2($C_{40}H_{66}B_2Cl_4Mo_4N_{12}O_{10}$)	$C_{97}H_{141}B_3Mo_3N_{29}O_6$	$C_{31}H_{38}BClMoN_7O_3$.$C_{13}H_{11}NO_2$	$C_{52}H_{70}B_2Mo_2N_{12}O_8S_2$	$C_{54}H_{74}B_2Mo_2N_{12}O_8S_2$.$C_7H_8$
formula mass	2844.46	2186.66	912.11	1268.82	1389.0
cryst syst	orthorhombic	triclinic	monoclinic	triclinic	triclinic
space group	$P2_12_12_1$	$P\bar{1}$	$P2_1/n$	$P\bar{1}$	$P\bar{1}$
a, Å	15.2184(13)	15.7509(2)	11.2514(15)	10.3391(92)	11.2230(11)
b, Å	19.0459(16)	19.4367(4)	21.978(3)	10.7247(96)	12.4901(13)
c, Å	39.415(3)	20.3448(4)	18.698(2)	14.6849(13)	13.8830(14)
α, deg	90	108.798(2)	90	94.130(16)	97.350(2)
β, deg	90	96.883(1)	107.51	107.839(15)	104.833(2)
γ, deg	90	102.2830(10)	90	106.667(16)	113.740(2)
V, Å^3	11424.5(17)	5640.51(18)	4409.5(10)	1642(2)	1662.3(3)
Z	8	2	4	1	1
ρ, gcm^{-3}	1.654	1.399	1.374	1.441	1.379
μ, cm^{-1}	11.05	4.90	4.12	5.62	5.01
data	25902	34527	10383	8534	10437
unique data	22226	13324	9272	6131	8228
R_1 [$I > 2\sigma(I)$][a]	0.0418	0.0746	0.0376	0.0766	0.0554
wR_2 (F_o^2, all data)[b]	0.1011	0.1597	0.0960	0.1807	0.1406
GoF	1.031	1.052	1.040	1.068	1.004

[a] $R_1 = \sum||F_o| - |F_c||/\sum|F_o|$. [b] $wR_2 = \{[\sum w(F_o^2 - F_c^2)^2/\sum(w|F_o^2|)^2]\}^{1/2}$.

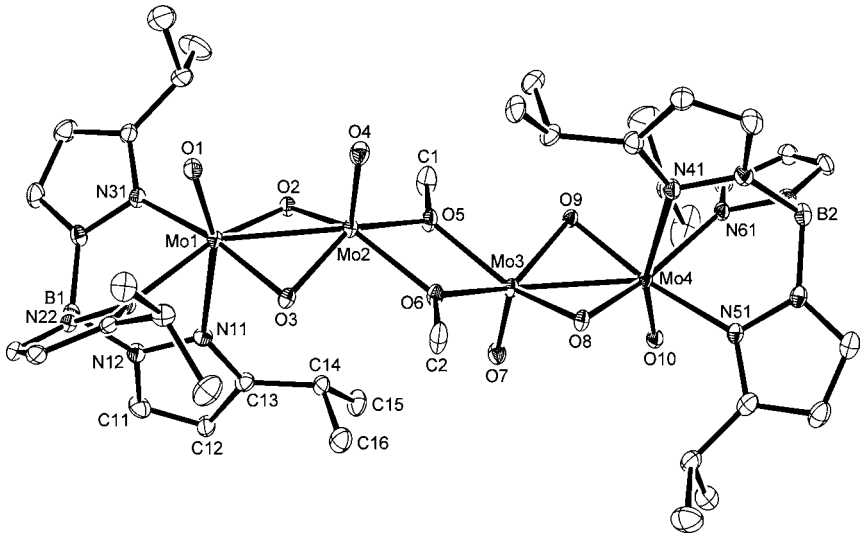

Figure 1. ORTEP representation of molecule A of **1** showing partial atom-labeling scheme and drawn at 30% ellipsoid probability. Hydrogen atoms are omitted for clarity.

dx.doi.org/10.1021/ic2026686 | *Inorg. Chem.* 2012, 51, 3202−3211

Table 2. Selected Bond Distances (Å) and Angles (Degrees) for Molecule A of 1[a]

		Bond Distances	
Mo(1)−O(1)	1.681(3) (1.670)	Mo(2)−O(3)	1.906(3) (1.901)
Mo(1)−O(2)	1.953(3) (1.956)	Mo(2)−O(4)	1.675(4) (1.668(3))
Mo(1)−O(3)	1.964(3) (1.955)	Mo(2)−O(5)	2.052(3) 2.059)
Mo(1)−N(11)	2.379(4) (2.387)	Mo(2)−O(6)	2.075(3) (2.070)
Mo(1)−N(21)	2.209(4) (2.197)	O(5)−C(1)	1.438(6) (1.428)
Mo(1)−N(31)	2.203(4) (2.198)	Mo(1)−Mo(2)	2.5478(6) (2.5457)
Mo(2)−O(2)	1.905(3) (1.914)	Mo(2)−Mo(3)	3.3587(6)
		Bond Angles	
O(1)−Mo(1)−O(2)	107.93(16) (108.97)	O(2)−Mo(2)−O(3)	93.80(14) (94.03)
O(1)−Mo(1)−O(3)	105.59(15) (104.33)	O(2)−Mo(2)−O(4)	108.83(16) (107.58)
O(1)−Mo(1)−N(11)	160.73(15) (161.39)	O(2)−Mo(2)−O(5)	87.14(14) (88.00(13))
O(1)−Mo(1)−N(21)	89.35(16) (90.33)	O(2)−Mo(2)−O(6)	144.43(14) (147.91)
O(1)−Mo(1)−N(31)	87.99(16) (87.44)	O(3)−Mo(2)−O(4)	111.11(16) (101.93)
O(2)−Mo(1)−O(3)	90.52(13) (91.06)	O(3)−Mo(2)−O(5)	141.29(14) (138.01)
O(2)−Mo(1)−N(11)	85.82(14) (84.32)	O(3)−Mo(2)−O(6)	87.00(13) (86.54)
O(2)−Mo(1)−N(31)	87.34(14) (87.34)	O(4)−Mo(2)−O(5)	105.07(16) (107.68(15))
O(3)−Mo(1)−N(11)	87.26(14) (87.94)	O(4)−Mo(2)−O(6)	103.91(16) (101.93)
O(3)−Mo(1)−N(21)	89.33(14) (89.62)	O(5)−Mo(2)−O(6)	71.07(13) (71.03)
O(3)−Mo(1)−N(31)	166.23(15) (159.86)	Mo(1)−O(2)−Mo(2)	82.66(13) (82.24)
N(11)−Mo(1)−N(21)	76.26(15) (75.59(14))	Mo(1)−O(3)−Mo(2)	82.32(13) (82.60)
N(11)−Mo(1)−N(31)	79.02(15) (80.04)	Mo(2)−O(5)−Mo(3)	109.15(15) (108.70)
N(21)−Mo(1)−N(31)	88.56(15) (87.82)	Mo(1)−Mo(2)−Mo(3)	150 (151)

[a]The second number (in parentheses) is the distance or angle pertaining to the (pseudo) inversion-center-related entity, e.g., the angle for O(1)−Mo(1)−O(2) is 107.93(16)°, while that for O(8)−Mo(4)−O(10) is 108.97(16)°. Unless stated, the esd of the second parameter is the same as that of the first.

Each dinuclear unit contains an $[Mo^{V}_2O_2(\mu\text{-}O)_2]^{2+}$ unit with two structurally distinct Mo centers; the peripheral $Tp^{iPr}Mo^{V}O(\mu\text{-}O)_2$ centers (Mo(1) and Mo(4)) are six coordinate (excluding the Mo−Mo interaction) and exhibit distorted octahedral geometries, while the central $Mo^{V}O(\mu\text{-}O)_2(\mu\text{-}OMe)_2$ units (Mo(2) and Mo(3)) are five coordinate and exhibit square pyramidal geometries.

Selected bond distances and angles for **1** are given in Table 2. The average bond distances for the terminal Mo═O and bridging Mo−O ligands are ca. 1.67 and 1.93 Å, respectively. The trans influence of the terminal oxo ligand results in a significant lengthening of the Mo−N(*n*1) (*n* = 1, 4) bonds relative to the other Mo−N bonds. The tetranuclear complex possesses alternating short Mo(1)−Mo(2) (∼2.55 Å), long Mo(2)−Mo(3) (∼3.36 Å), and short Mo(3)−Mo(4) (∼2.55 Å) metal−metal distances; the short Mo−Mo bond lengths are indicative of an Mo−Mo single bond in each of the dinuclear units. These features are observed in other closely related tetranuclear species, e.g., $[TpMoO(\mu\text{-}O)_2MoO(MeOH)]_2(\mu\text{-}OMe)_2$ (Tp = hydrotris(pyrazol-1-yl)borate)[25] and $[Tp^{*}MoO(\mu\text{-}O)_2MoO]_2(\mu\text{-}OH)_2$ (Tp* = hydrotris(3,5-dimethylpyrazol-1-yl)borate).[26]

Complex **1** adopts a zigzag conformation with Mo(1)−Mo(2)···Mo(3) and Mo(2)···Mo(3)−Mo(4) angles of ca. 150° and 151°, respectively. These values are significantly greater than those reported for $[TpMoO(\mu\text{-}O)_2MoO(MeOH)]_2(\mu\text{-}OMe)_2$ (ca. 127°),[25] where the central Mo atoms are six coordinate and coordinated by a methanol ligand cis to the oxo ligands. The peripheral $Mo_2(\mu\text{-}O)_2$ units adopt a butterfly configuration, while the central $Mo_2(\mu\text{-}OMe)_2$ unit is almost planar, with rms atom displacements of 0.0152 and 0.0065 Å for molecules A and B, respectively.

Reactions of Ketone Complexes with Methylamine. Generation of a water molecule *at* (or near) the Mo center would enhance formation of an aqua or a hydroxo complex, provided H-bond stabilization of the complex is competitive with phenolate ligand chelation. However, in the Schiff base condensation of $Tp^{iPr}MoO\{OC_6H_4C(O)Me\}$ with methylamine (eq 1), chelation, and formation of $Tp^{iPr}MoO\{OC_6H_4C(Me)NMe\text{-}\kappa^2O,N\}$ (**2**) predominates.

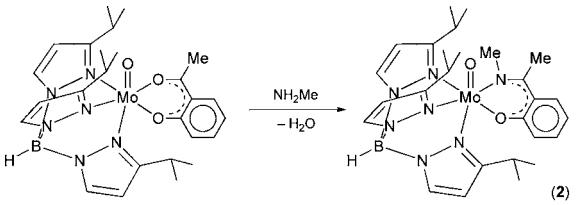

(1)

The IR spectrum of **2** exhibited bands assignable to ν(Mo═O) and ν(C═N) stretching modes at 953 and 1599 cm^{-1}, respectively. No resonances indicative of the presence of an aqua ligand were observed in the ^1H NMR spectrum of the complex. An analogous reaction between $Tp^{iPr}MoO\{OC_6H_4C(O)Et\}$ and methylamine did not yield tractable products.

The identity of the complex was confirmed by the X-ray crystal structure of **2**·3MeCN, which revealed an asymmetric unit containing three independent molecules of **2** (Figure 2) and nine acetonitrile molecules; metrical parameters for **2** are presented in Table 3. Complexes **2** exhibit distorted octahedral geometries and feature a terminal oxo ligand, a bidentate iminophenolate ligand, and a tridentate *fac*-Tp^{iPr} ligand. In each independent molecule, the Mo atom is displaced ca. 0.31 Å from the equatorial plane in the direction of the terminal oxo ligand. The average Mo═O and Mo−O distances of 1.686 and 2.046 Å, respectively, are typical of related oxo(phenolate)−Mo(IV) complexes.[18] The average $Mo-N_{imine}$ distance is comparable to the equatorial $Mo-N_{Tp}$ distances, whereas the $Mo-N_{Tp}$ bonds trans to the oxo ligands are lengthened by the strong trans influence

dx.doi.org/10.1021/ic2026686 | Inorg. Chem. 2012, 51, 3202−3211

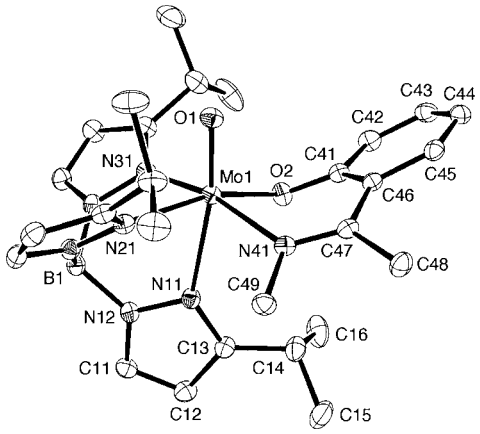

Figure 2. ORTEP projection of molecule 1 of **2** showing a partial atom-labeling scheme and drawn at 30% ellipsoid probability. Hydrogen atoms are omitted for clarity.

of the oxo ligand. The six-membered chelate ring is nonplanar, the phenolate ring being tilted significantly toward the terminal oxo ligand (ca. 43°). This results in the imine carbon atom being displaced significantly from the plane of the phenolate and imine nitrogen donor (ca. 0.28 Å), the torsion angles, e.g., for N(41)−C(47)−C(46)−C(41), being ca. 26°.

Oxidation Reactions. As demonstrated by generation of **1** (vide supra), the oxo−Mo(IV) complexes are thermodynamically unstable with respect to oxidation. For convenience, the other oxidation reactions observed for these complexes are collected and described in the sections that follow.

Reactions with Hydrogen Peroxide. The title complexes were rapidly and quantitatively oxidized by hydrogen peroxide to yield the dioxo−Mo(VI) precursors (eq 2). The dioxo−Mo(VI) complexes were very slowly formed upon reaction with oxygen in the air.

$$Tp^{iPr}Mo^{IV}O(OAr{-}R) + H_2O_2 \rightarrow Tp^{iPr}Mo^{VI}O_2(OAr{-}R) + H_2O \quad (2)$$

Reactions with Dichloromethane. The title complexes reacted with chlorinated solvents (e.g., dichloromethane) under anaerobic conditions to give oxo−Mo(V) chloro species (likely formed via eqs 3 and 4). These deep purple complexes were observed by EPR spectroscopy ($g_{iso} \approx 1.939$). Chlorine atom transfer reactions have been observed in previous studies involving oxo−Mo(IV) scorpionate complexes.[21,27,28]

$$Tp^{iPr}Mo^{IV}O(OAr{-}R) + CH_2Cl_2 \rightarrow Tp^{iPr}Mo^{V}OCl(OAr{-}R) + \bullet CH_2Cl \quad (3)$$

$$2 \bullet CH_2Cl \rightarrow CH_2ClCH_2Cl \quad (4)$$

Extended stirring and/or heating of the reaction mixtures resulted in further transformation of $Tp^{iPr}Mo^{V}OCl\{OC_6H_4C(O)R\}$ into $Tp^{iPr}Mo^{V}OCl_2$, the phenolate coligand being replaced by a second chloro ligand. This observation was derived from EPR experiments

Table 3. Selected Bond Distances (Å) and Angles (Degrees) for Molecules 1−3 of 2

parameter[a]	molecule 1	molecule 2	molecule 3
	Bond Distances		
Mo(1)−O(1)	1.6857(15)	1.6844(15)	1.6872(14)
Mo(1)−O(2)	2.0508(16)	2.0434(14)	2.0434(15)
Mo(1)−N(41)	2.1610(17)	2.1697(18)	2.1728(18)
Mo(1)−N(11)	2.4071(18)	2.3978(17)	2.4063(17)
Mo(1)−N(21)	2.2006(19)	2.1962(17)	2.2031(18)
Mo(1)−N(31)	2.1743(18)	2.1664(19)	2.1702(17)
O(2)−C(41)	1.320(3)	1.321(3)	1.325(3)
N(41)−C(47)	1.296(3)	1.300(3)	1.297(3)
	Bond Angles		
Mo(1)−O(2)−C(41)[a]	119.34(13)	118.99(13)	117.93(13)
Mo(1)−N(41)−C(47)	122.63(14)	122.99(15)	122.38(15)
O(1)−Mo(1)−O(2)	104.86(10)	107.60(7)	107.41(7)
O(1)−Mo(1)−N(41)	101.91(7)	102.65(7)	101.78(7)
O(1)−Mo(1)−N(11)	170.01(7)	169.24(7)	168.56(7)
O(1)−Mo(1)−N(21)	91.67(7)	91.26(7)	90.96(7)
O(1)−Mo(1)−N(31)	94.78(7)	94.89(8)	94.22(7)
O(2)−Mo(1)−N(41)	83.20(7)	83.30(6)	82.67(6)
O(2)−Mo(1)−N(11)	83.30(7)	81.39(6)	81.98(6)
O(2)−Mo(1)−N(21)	163.35(7)	160.91(6)	161.43(6)
O(2)−Mo(1)−N(31)	88.95(7)	87.69(7)	88.05(6)
N(41)−Mo(1)−N(11)	84.58(6)	83.96(6)	85.65(6)
N(41)−Mo(1)−N(21)	95.55(7)	95.71(7)	96.46(7)
N(41)−Mo(1)−N(31)	162.89(7)	162.02(7)	163.30(7)
N(11)−Mo(1)−N(21)	80.06(6)	79.55(6)	79.47(6)
N(11)−Mo(1)−N(31)	79.40(7)	79.31(7)	79.30(6)
N(21)−Mo(1)−N(31)	87.63(7)	87.75(7)	87.93(7)
Mo−(O_3)[b]	1.966	1.966	1.968
Mo−(N_3)[c]	2.261	2.253	2.260
Mo−equatorial[d]	0.3076(11)	0.3340(10)	0.3141(10)

[a]Atom numbers apply to molecule 1 only (corresponding distances and angles given for other molecules). [b]The average Mo−O/N distance. [c]The average Mo−N(pyrazole) distance. [d]The displacement of the Mo atom from the equatorial plane defined by N(21), N(31), N(41), and O(2).

dx.doi.org/10.1021/ic2026686 | Inorg. Chem. 2012, 51, 3202−3211

where the signal from the precursor was slowly replaced by a new signal at g_{iso} = 1.949, characteristic of $Tp^{iPr}Mo^{V}OCl_2$.[21]

Reactions with Ferrocenium Tetrafluoroborate. Oxidation of $Tp^{iPr}MoO\{OC_6H_4C(O)R\}$ by $[FeCp_2]BF_4$ (eq 5) was examined to assess the feasibility of displacing the carbonyl moiety by water or hydroxyl anions at the Mo(V) oxidation level. A large excess of the oxidizing reagent was used to drive the reactions to completion. All reactions produced a single product that exhibited an Mo(V) EPR signal at ca. 1.942.

$$Tp^{iPr}MoO(OAr{-}R) + [FeCp_2]BF_4 \rightarrow [Tp^{iPr}MoO(OAr{-}R)]BF_4 + FeCp_2 \quad (5)$$

These oxo−Mo(V) species did not react with deoxygenated water even with prolonged reaction times. However, they did react with excess NBu^{n}_4OH to give the corresponding *cis*-dioxo−Mo(V) radical anions, $[Tp^{iPr}MoO_2\{OC_6H_4C(O)R\}]^-$. Oxo(hydroxo)−Mo(V) intermediates were not observed, presumably because of their instantaneous deprotonation by excess base. A proposed reaction sequence is presented in eq 6. Interestingly, no reactions were observed with stoichiometric amounts of NBu^{n}_4OH.

$$[Tp^{iPr}MoO(OAr{-}R)]^+ + 2OH^- \rightarrow \{Tp^{iPr}MoO(OH)(OAr{-}R)\}^{\ddagger} + OH^- \rightarrow [Tp^{iPr}MoO_2(OAr{-}R)]^- + H_2O \quad (6)$$

Reactions with Ammoniumyl Hexachloroantimonate. Oxidation of the title complexes using strong oxidizing agents, including Ag(I) and nitrosonium salts, was trialled but yielded intractable reaction mixtures. Use of ammoniumyl salts, such as $[N(4\text{-}C_6H_4Br)_3][SbCl_6]$, as oxidizing agents was then investigated, as these have the required reduction potentials, viz., ca. +0.7 V (+0.70 V Fc^+/Fc in CH_2Cl_2; +0.67 V vs Fc^+/Fc in CH_3CN).[19] Trial reactions carried out on the EPR scale proved successful, yielding results similar to those of the ferrocenium oxidations described above. Preparative-scale reactions were carried out using $Tp^{iPr}MoO(OC_6H_4CO_2Me)$ and $Tp^{iPr}MoO\{OC_6H_4C(O)Me\}$.

Golden-brown $[Tp^{iPr}MoO\{OC_6H_4C(O)R\}][SbCl_6]$ (R = OMe (**3**) and Me (**4**)) were synthesized from the stoichiometric reaction of the appropriate Mo(IV) derivative with $[N(4\text{-}C_6H_4Br)_3][SbCl_6]$ in dichloromethane according to eq 7. These reactions were quite rapid and were complete within 1 h. The reaction mixture was evaporated to dryness and extracted with toluene to remove the amine byproduct. The Mo complexes are soluble in polar (e.g., THF, CH_3CN) and chlorinated solvents but only sparingly soluble in hexane, toluene, and diethyl ether. These complexes are unstable and readily hydrolyzed in the presence of atmospheric moisture to oxo−Mo(V) chloro complexes (eq 8; *not balanced*). The solids also appear to be thermally unstable, decomposing over time. Consequently, they should be stored under inert conditions at low temperatures.

$$Tp^{iPr}Mo^{IV}O(OAr{-}R) + [NAr'_3][SbCl_6] \rightarrow [Tp^{iPr}Mo^{V}O(OAr{-}R)][SbCl_6] + NAr'_3 \quad (7)$$

$$[Tp^{iPr}MoO\{OC_6H_4C(O)NHPh\}][SbCl_6] \rightarrow Tp^{iPr}Mo^{V}OCl\{OC_6H_4C(O)NHPh\} + 2\text{-}HOC_6H_4C(O)NHPh + Sb(OH)_n \quad (8)$$

Both **3** and **4** were characterized using a variety of techniques, including EPR and IR spectroscopies and mass spectrometry. Decomposition prevented collection of accurate microanalyses, while disorder complicated X-ray crystallographic studies. In one instance, the decomposition product of $[Tp^{iPr}MoO\{OC_6H_4C(O)NHPh\}][SbCl_6]$ (eq 8) was obtained and structurally characterized as **5**.

The complex in **5** displays a distorted octahedral geometry defined by tridentate *fac*-Tp^{iPr} and mutually cis monodentate oxo, chloro, and phenolate ligands (Figure 3). A molecule of

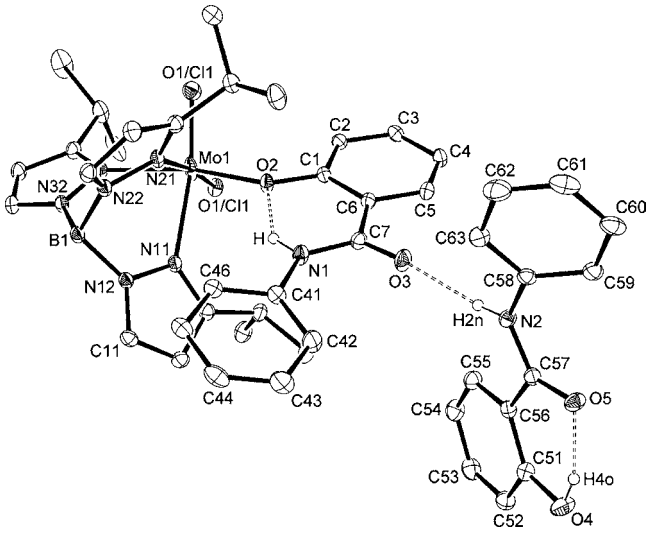

Figure 3. ORTEP projection of **5** showing a partial atom-labeling scheme and drawn at 30% ellipsoid probability. Hydrogen atoms (except for H, H(2n), and H(4o)) are omitted for clarity.

the protonated coligand, 2-phenylsalicylanilide, is also present in the crystal lattice; its presence is indicative of complex decomposition pathways. Due to positional disorder of the oxo and chloro ligands, the observed Mo=O and Mo−Cl distances of ca. 1.80 and 2.21 Å, respectively, are unreliable (the former being lengthened and the latter shortened as a consequence of disorder). The $Mo-O_{OAr}$ bond distance of 1.9598(12) Å is comparable to those found in related dioxo−Mo(VI) complexes.[20] There are several H bonds present in the solid-state structure of **5**. These include intramolecular H bonds, N(1)−H···O(2) and O(4)−H(4o)···O(5), and intermolecular H bond N(2)−H(2n)···O(3). Of these, the N(1)−H···O(2) bond angle shows the largest deviation from 180°, due to its incorporation into the rigid six-membered ring defined by N(1), H, O(2), C(1), C(6), and C(7). Selected bond distances and angles and a complete listing of the H-bond parameters for **5** can be found in the Supporting Information.

Reactions with Propylene Sulfide. Dark red-brown $Tp^{iPr}MoOS\{OC_6H_4C(O)R\}$ (**6**−**8**) were synthesized upon sulfur atom abstraction from propylene sulfide according to eq 9. The isolated solids may be handled briefly in air but prolonged exposure results in formation of *cis*-$Tp^{iPr}MoO_2\{OC_6H_4C(O)R\}$ and $[Tp^{iPr}MoO]_2(\mu\text{-}O)(\mu\text{-}S_2)$.[29] Purification was achieved by recrystallization from either THF/hexane or toluene/hexane mixtures or by column chromatography. Optimized syntheses are reported; longer reaction times or gentle heating only resulted in formation of $Tp^{iPr}MoO\{OSC_6H_3C(O)R\text{-}\kappa^2O,S\}$ (as indicated by EPR spectroscopy ($g_{iso} \approx$ 1.956)).[29] Although monomeric in solution, the complexes

dx.doi.org/10.1021/ic2026686 | *Inorg. Chem.* 2012, 51, 3202−3211

crystallize as dimeric, μ-disulfido−Mo(V) species, $[Tp^{iPr}MoO\{OC_6H_4C(O)R\}]_2(\mu\text{-}S_2)$ (**6**−**8** refers to both forms). It should also be noted that the phosphine adducts, $Tp^{iPr}MoO\{OC_6H_4C(O)NHPh\}\cdot PR'_3$,[18] were stable in the presence of propylene sulfide. All other oxo−Mo(IV) precursors gave intractable brown oils upon reaction with propylene sulfide.

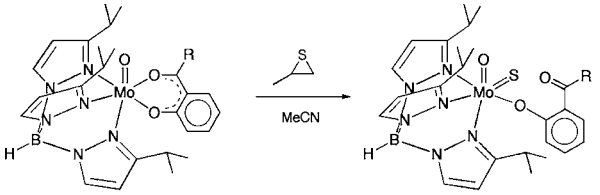

(9)

The IR (KBr) spectra of *as-isolated* **6**−**8** indicated the presence of both monomeric and dimeric species in the solid state; however, only crystals of the dimeric complexes were obtained from crystal growth experiments. In solution (CH_2Cl_2), the monomeric species were exclusively present. To date, it has not been possible to isolate the monomer in the absence of contamination from the dimer. The $\nu(Mo^{V}{=}O)$ stretching modes for the dimeric complexes were observed at ca. 940 cm^{-1}, a ν(Mo═S) band being absent. In contrast, the monomeric species exhibited strong bands at ca. 915 and 485 cm^{-1}, which were assigned to the $\nu(Mo^{VI}{=}O)$ and $\nu(Mo^{VI}{=}S)$ modes, respectively, of the *cis*-oxosulfido−Mo(VI) moiety; the positions and intensities of these bands were consistent with literature values for related complexes.[29] Significantly, these values are comparable to the stretching frequencies of the Mo═O and Mo═S groups of bovine xanthine oxidase (899 and 474 cm^{-1}, respectively).[30] The carbonyl functional groups give rise to characteristic bands at ca. 1690−1745 cm^{-1}, close to the values reported for the analogous *cis*-dioxo−Mo(VI) complexes.[20] Bands characteristic of the Tp^{iPr} (ν(BH) 2521−2458 cm^{-1}, ν(CN) ca. 1507 cm^{-1}) and phenolate (ν(CO) ca. 1570 cm^{-1} and $\nu(CC)_{ring}$ ca. 1260 cm^{-1}) ligands were also present.[31] The substitution patterns of the phenol coligands are well represented in the fingerprint region (900−680 cm^{-1}), with CH out-of-plane bending modes corresponding to a monosubstituted aromatic ring.[32]

Unlike their alkyl- and aryl-substituted counterparts, $Tp^{iPr}MoOS(OAr{-}R)$ (R = H, alkyl, aryl),[29,33] the ester-substituted complexes **6**−**8** exhibited highly fluxional ^{1}H NMR behavior, leading to broad or absent NMR signals at room temperature. Low-temperature NMR spectra revealed the presence of multiple species, probably due to fluxional processes *and* temperature-dependent monomer−dimer equilibria. The variable-temperature NMR behavior of the complexes was not investigated.

Complexes **6**−**8** (monomer forms) exhibited a single, reversible, one-electron reduction (eq 10) in the potential range from −0.475 to −0.450 V vs SCE in acetonitrile. These reduction potentials compare favorably with those reported for related complexes by Doonan et al.[29] No other electrochemical processes were observed. Consistent with diffusion-controlled redox processes,[34] the $E_{1/2}$ values were independent of scan rates, peak current ratios were close to unity, and plots of current vs $\nu^{1/2}$ (where ν is the scan rate) were strictly linear.

$$Tp^{iPr}Mo^{VI}OS(OAr{-}R) + e^- \rightarrow [Tp^{iPr}Mo^{V}OS(OAr{-}R)]^- \quad (10)$$

The reduction potentials for these *cis*-oxosulfido−Mo(VI) complexes are all significantly more positive than those observed for their *cis*-dioxo−Mo(VI) counterparts (ΔE > 300 mV) due to the lower energy of the LUMO (and relative ease of reduction) in the $[MoOS]^{2+}$ complexes compared to the $[MoO_2]^{2+}$ complexes. This observation is consistent with the electrochemical behavior of related Mo[29] and W[35] complexes and pseudo-tetrahedral complexes such as $MoO_2(ONR_2)_2$ and $MoOS(ONR_2)_2$ (NR_2 = piperidine).[36,37]

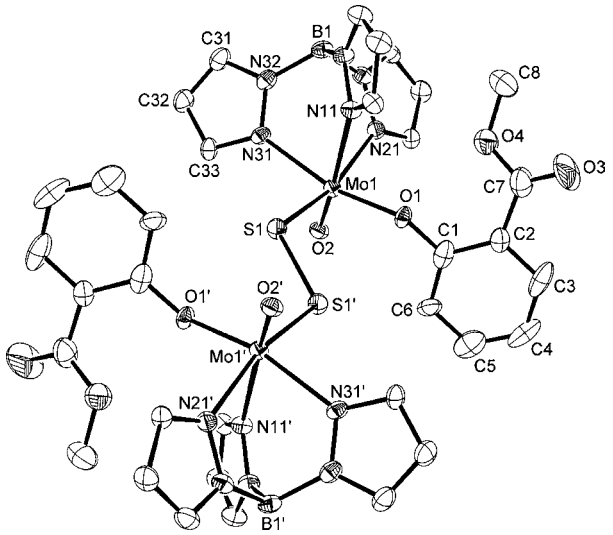

Figure 4. ORTEP projection of **6** showing a partial atom-labeling scheme and drawn at 30% ellipsoid probability. Hydrogen atoms and isopropyl groups of Tp^{iPr} are omitted for clarity.

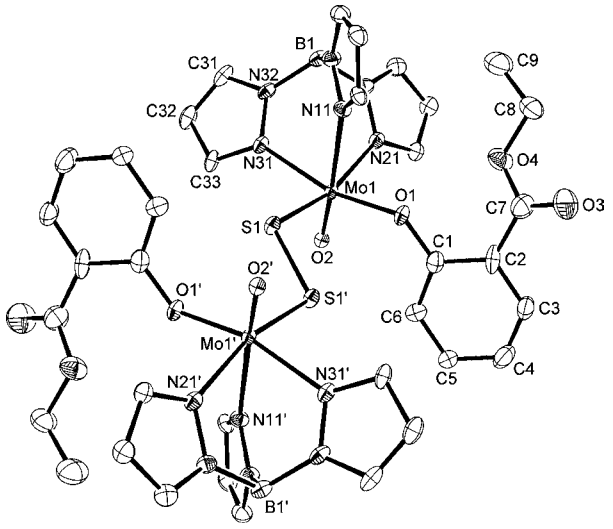

Figure 5. ORTEP projection of **7** showing a partial atom-labeling scheme and drawn at 30% ellipsoid probability. Hydrogen atoms and isopropyl groups of Tp^{iPr} are omitted for clarity.

Dimeric **6** (Figure 4) and **7** (Figure 5) exhibit centrosymmetric structures and metrical parameters (Table 4) closely related to those reported for $[Tp^{iPr}MoO(OPh)]_2(\mu\text{-}S_2)$[33] and $[Tp^{iPr}MoO(3,5\text{-}OC_6H_3{}^tBu_2)]_2(\mu\text{-}S_2)$.[29] The Mo centers in **6** and **7** adopt distorted octahedral geometries and are coordinated by a facial, tridentate Tp^{iPr} ligand and mutually cis

dx.doi.org/10.1021/ic2026686 | Inorg. Chem. 2012, 51, 3202−3211

Table 4. Selected Bond Distances (Å) and Angles (Degrees) for Complexes 6 and 7

parameter	6	7
Bond Distances		
Mo(1)−O(2)	1.690(5)	1.691(3)
Mo(1)−S(1)	2.336(3)	2.3587(11)
Mo(1)−O(1)	1.942(4)	1.949(3)
Mo(1)−N(11)	2.373(6)	2.350(3)
Mo(1)−N(21)	2.255(6)	2.233(3)
Mo(1)−N(31)	2.209(6)	2.208(3)
S(1)−S(1′)	2.091(4)	2.106(2)
O(1)−C(1)	1.344(9)	1.373(5)
O(3)−C(7)	1.176(11)	1.235(7)
Bond Angles		
O(1)−Mo(1)−S(1)	94.75(15)	96.30(9)
O(1)−Mo(1)−O(2)	103.1(2)	102.10(13)
O(1)−Mo(1)−N(11)	83.7(2)	85.06(12)
O(1)−Mo(1)−N(21)	91.3(2)	88.93(12)
O(1)−Mo(1)−N(31)	163.9(2)	164.62(12)
O(2)−Mo(1)−S(1)	101.92(16)	102.22(10)
O(2)−Mo(1)−N(11)	167.3(2)	167.98(13)
O(2)−Mo(1)−N(21)	91.0(2)	91.10(13)
O(2)−Mo(1)−N(31)	92.2(2)	91.45(13)
S(1)−Mo(1)−N(11)	88.08(15)	86.37(9)
S(1)−Mo(1)−N(21)	164.08(16)	164.26(9)
S(1)−Mo(1)−N(31)	87.10(16)	87.78(9)
N(11)−Mo(1)−N(21)	78.0(2)	79.29(12)
N(11)−Mo(1)−N(31)	80.4(2)	80.38(12)
N(21)−Mo(1)−N(31)	83.1(2)	83.51(12)
Mo(1)−S(1)−S(1′)	109.05(14)	109.09(7)
Mo(1)−O(1)−C(1)	143.2(5)	135.9(3)

terminal oxo, phenolate, and bridging μ-disulfido-κS:$\kappa S'$ ligands. The terminal oxo ligands assume an anti disposition across the S−S bridge. The short Mo(1)−O(2) distances of ca. 1.69 Å are typical of terminal Mo═O bonds, while the long Mo(1)−S(1) and Mo(1)−O(1) bond lengths of ca. 2.35 and 1.95 Å, respectively, are characteristic of Mo−S/O single bonds.[38] The Mo(1)−N(11), Mo(1)−N(21), and Mo(1)−N(31) bond distances of ca. 2.36, 2.24, and 2.21 Å, respectively, reflect the relative trans influences of the coligands, viz., oxo ≫ μ-disulfido > phenoxy. The S(1)−S(1′) distance of ca. 2.10 Å is consistent with the presence of an S−S single bond.[38]

The O(2)−Mo(1)−S(1) angles are 101.92(16)° and 102.22(10)° for complexes **6** and **7**, respectively, close to values reported for related species.[29,33] The obtuse N(31)−Mo(1)−O(1) and N(21)−Mo(1)−S(1) angles of ca. 164° constitute the greatest deviations from ideal octahedral geometry. In the solid state, the phenolate ring is proximal to the terminal oxo ligands and the 2-R substituents are directed toward a cleft in the Tp^{iPr} ligand, being nestled between the two isopropyl groups "opposite" the oxo ligand. The molecules exhibit Mo(1)−O(1)−C(1) angles of 143.2(5)° and 135.9(3)°, which are within the ranges observed for *cis*-dioxo−Mo(VI) complexes sharing the same phenolate ligand conformation.[20]

SUMMARY

The oxo−Mo(IV) title complexes are generally stable toward water and do not serve as precursors for oxo(aqua)−Mo(IV) species; rather, tetranuclear or chelated iminophenolate complexes are preferentially formed from the complexes and water (generated by Schiff base condensation in the latter case). The title complexes are readily oxidized by dioxygen and hydrogen peroxide to generate the corresponding *cis*-dioxo−Mo(VI) compounds. In addition, suitable one-electron oxidants, e.g., $[FeCp_2]$-BF_4 and $[N(4\text{-}C_6H_4Br)_3][SbCl_6]$, oxidize the complexes to their oxo−Mo(V) counterparts. Ester derivatives were found to be useful precursors for new *cis*-oxosulfido−Mo(VI) complexes upon sulfur atom transfer.

Thus, although the title complexes participate in well-established oxygen[4−6] and sulfur[29] atom transfer reactions, they do not provide access to stable, isolable, oxo(aqua)− or oxo(hydroxo)−Mo(IV/V) species.[6,8] Such species appear to be thermodynamically unstable with respect to ligand competition, one- and two-electron oxidation, or more complex degradation reactions, leading to isolation of the products described herein (Scheme 1). Indeed, the high intrinsic *E*/pH-dependent reactivity of the oxo(aqua)−Mo(IV) state of some Mo enzymes, e.g., "di-oxo" Mo enzymes such as sulfite oxidase, may facilitate efficient active site regeneration via one-electron, coupled electron−proton transfer processes; this in turn may account for the efficacy of these enzymes and the inherent difficulties in generating and studying their Mo(IV) state(s).[7−9] The stabilization and isolation of oxo(aqua)−Mo(IV) and (in pure form) oxo(hydroxo)−Mo(V)[12−15] complexes as models for the reduced states of Mo enzymes remains an elusive goal.

ASSOCIATED CONTENT

Supporting Information

Crystallographic data in CIF format (for all compounds) and tables of selected distances and angles for disordered **5**. This material is available free of charge via the Internet at http://pubs.acs.org.

AUTHOR INFORMATION

Corresponding Author

*E-mail: cgyoung@unimelb.edu.au.

Present Address

[†]Department of Chemistry, University of New England, Armidale, NSW 2351, Australia.

Notes

The authors declare no competing financial interest.

ACKNOWLEDGMENTS

We thank Ms. Low Xin Lian for experimental assistance and gratefully acknowledge financial support from the Australian Research Council, the Donors of the Petroleum Research Fund (administered by the American Chemical Society), and the Albert Shimmins Memorial Fund (for a writeup grant to V.N.).

REFERENCES

(1) Stiefel, E. I. *Prog. Inorg. Chem.* **1977**, *22*, 1−223.

(2) Garner, C. D.; Charnock, J. M. In *Comprehensive Coordination Chemistry*; Wilkinson, G., Gillard, R. D., McCleverty, J. A., Eds.; Pergamon: Oxford, 1987; Chapter 36.4, pp 1329−1374.

(3) Young, C. G. In *Comprehensive Coordination Chemistry II*; McCleverty, J. A., Meyer, T. J., Eds.; Elsevier-Pergamon: Amsterdam, 2004; Chapter 4.7, pp 415−527.

(4) Holm, R. H. *Chem. Rev.* **1987**, *87*, 1401−1449.

(5) Holm, R. H. *Coord. Chem. Rev.* **1990**, *100*, 183−221.

(6) Young, C. G. In *Biomimetic Oxidations Catalyzed by Transition Metal Complexes*; Meunier, B., Ed.; Imperial College Press: London, 2000; pp 415−459.

(7) Tunney, J. M.; McMaster, J.; Garner, C. D. In *Comprehensive Coordination Chemistry II*; McCleverty, J. A., Meyer, T. J., Eds.; Elsevier-Pergamon: Amsterdam, 2004; Chapter 8.18, pp 459−477.
(8) Young, C. G. In *Encyclopedia of Inorganic Chemistry 2*; King, R. B., Ed. Wiley: Chichester, U.K., 2005; pp 3321−3340.
(9) Romão, M. J. *Dalton Trans.* **2009**, 4053−4068.
(10) Kisker, C.; Schindelin, H.; Pacheco, A.; Wehbi, W. A.; Garrett, R. M.; Rajagopolan, K. V.; Enemark, J. H.; Rees, D. C. *Cell* **1997**, *91*, 973−976.
(11) Fischer, K.; Barbier, G. G.; Hecht, H.-J.; Mendel, R. R.; Campbell, W. H.; Schwarz, G. *Plant Cell* **2005**, *17*, 1167−1179.
(12) Xiao, Z.; Bruck, M. A.; Doyle, C.; Enemark, J. H.; Grittini, C.; Gable, R. W.; Wedd, A. G.; Young, C. G. *Inorg. Chem.* **1995**, *34*, 5950−5962; Erratum: *ibid.* **1996**, *35*, 5752.
(13) Xiao, Z.; Gable, R. W.; Wedd, A. G.; Young, C. G. *J. Am. Chem. Soc.* **1996**, *118*, 2912−2921.
(14) Ng, V. W. L.; Taylor, M. K.; White, J. M.; Young, C. G. *Inorg. Chem.* **2010**, *49*, 9460−9469.
(15) Young, C. G.; Laughlin, L. J.; Colmanet, S.; Scrofani, S. D. B. *Inorg. Chem.* **1996**, *35*, 5368−5377.
(16) Xiao, Z.; Bruck, M. A.; Enemark, J. H.; Young, C. G.; Wedd, A. G. *Inorg. Chem.* **1996**, *35*, 7508−7515.
(17) Woo, L. K. *Chem. Rev.* **1993**, *93*, 1125−1136.
(18) Ng, V. W. L.; Taylor, M. K.; Hill, L. M. R.; White, J. M.; Young, C. G. *Eur. J. Inorg. Chem.* **2010**, 3261−3269.
(19) Connelly, N. G.; Geiger, W. E. *Chem. Rev.* **1996**, *96*, 877−910.
(20) Hill, L. M. R.; Taylor, M. K.; Ng, V. W. L.; Young, C. G. *Inorg. Chem.* **2008**, *47*, 1044−1052.
(21) Millar, A. J.; Doonan, C. J.; Laughlin, L. J.; Tiekink, E. R. T.; Young, C. G. *Inorg. Chim. Acta* **2002**, *337*, 393−406.
(22) Sheldrick, G. M. *SHELXS-97, Program for Crystal Structure Solution*; University of Göttingen: Göttingen, Germany, 1997.
(23) Sheldrick, G. M. *SHELXL-97, Program for Crystal Structure Refinement*; University of Göttingen: Göttingen, Germany, 1997.
(24) Farrugia, L. J. *J. Appl. Crystallogr.* **1997**, *30*, 565.
(25) (a) Koch, S. A.; Lincoln, S. *Inorg. Chem.* **1982**, *21*, 2904−2905. (b) Lincoln, S; Koch, S. A. *Inorg. Chem.* **1986**, *25*, 1594−1602.
(26) Kisala, J.; Bialonska, A.; Ciunik, Z.; Kurek, S.; Wolowiec, S. *Polyhedron* **2006**, *25*, 3222−3230.
(27) Roberts, S. A.; Young, C. G.; Kipke, C. A.; Cleland, W. E. Jr.; Yamanouchi, K.; Carducci, M. D.; Enemark, J. H. *Inorg. Chem.* **1990**, *29*, 3650−3656.
(28) Xiao, Z.; Bruck, M. A.; Enemark, J. H.; Young, C. G.; Wedd, A. G. *J. Biol. Inorg. Chem.* **1996**, *1*, 415−423.
(29) Doonan, C. J.; Nielsen, D. J.; Smith, P. D.; White, J. W.; George, G. N.; Young, C. G. *J. Am. Chem. Soc.* **2006**, *128*, 305−316.
(30) Maiti, N. C.; Tomita, T.; Kitagawa, T.; Okamoto, K.; Nishino, T. *J. Biol. Inorg. Chem.* **2003**, *8*, 327−333.
(31) Silverstein, R. M.; Bassler, C. G.; Morrill, T. C. *Spectrophotometric Identification of Organic Compounds*, 4th ed.; Wiley: New York, 1981.
(32) Williams, D. H.; Fleming, I. *Spectroscopic Methods in Organic Chemistry*, 5th ed.; McGraw-Hill: London, 1995.
(33) Smith, P. D.; Slizys, D. A.; George, G. N.; Young, C. G. *J. Am. Chem. Soc.* **2000**, *122*, 2946−2947.
(34) Christensen, P. A.; Hamnett, A. *Techniques and Mechanisms in Electrochemistry*; Chapman and Hall: Oxford, 1994.
(35) Eagle, A. A.; Tiekink, E. R. T.; George, G. N.; Young, C. G. *Inorg. Chem.* **2001**, *40*, 4563−4573.
(36) Bristow, S.; Garner, C. D.; Pickett, C. J. *J. Chem. Soc., Dalton Trans.* **1984**, 1617−1619.
(37) Traill, P. R.; Bond, A. M.; Wedd, A. G. *Inorg. Chem.* **1994**, *33*, 5754−5760.
(38) Orpen, A. G.; Brammer, L.; Allen, F. H.; Kennard, O.; Watson, D. G.; Taylor, R. *J. Chem. Soc., Dalton Trans.* **1989**, S1−S83.